

# Fucose–Galactose Polymers Inhibit Cholera Toxin Binding to Fucosylated Structures and Galactose-Dependent Intoxication of Human Enteroids

Jakob Cervin, Andrew Boucher, Gyusaang Youn, Per Björklund, Ville Wallenius, Lynda Mottram, Nicole S. Sampson, and Ulf Yrlid\*



Cite This: *ACS Infect. Dis.* 2020, 6, 1192–1203



Read Online

ACCESS |



Metrics & More



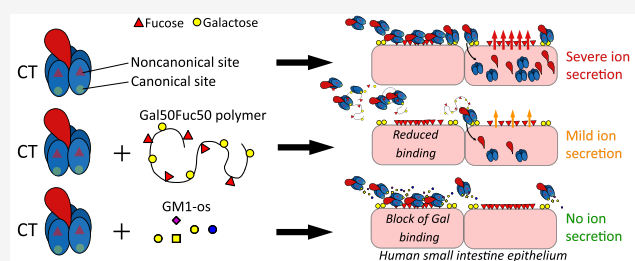
Article Recommendations



Supporting Information

**ABSTRACT:** A promising strategy to limit cholera severity involves blockers mimicking the canonical cholera toxin ligand (CT) ganglioside GM1. However, to date the efficacies of most of these blockers have been evaluated in noncellular systems that lack ligands other than GM1. Importantly, the CT B subunit (CTB) has a noncanonical site that binds fucosylated structures, which in contrast to GM1 are highly expressed in the human intestine. Here we evaluate the capacity of norbornene polymers displaying galactose and/or fucose to block CTB binding to immobilized protein-linked glycan structures and also to primary human and murine small intestine epithelial cells (SI ECs). We show that the binding of CTB to human SI ECs is largely dependent on the noncanonical binding site, and interference with the canonical site has a limited effect while the opposite is observed with murine SI ECs. The galactose–fucose polymer blocks binding to fucosylated glycans but not to GM1. However, the preincubation of CT with the galactose–fucose polymer only partially blocks toxic effects on cultured human enteroid cells, while preincubation with GM1 completely blocks CT-mediated secretion. Our results support a model whereby the binding of fucose to the noncanonical site places CT in close proximity to scarcely expressed galactose receptors such as GM1 to enable binding via the canonical site leading to CT internalization and intoxication. Our finding also highlights the importance of complementing CTB binding studies with functional intoxication studies when assessing the efficacy inhibitors of CT.

**KEYWORDS:** cholera toxin, norbornene, fucose, galactose, multivalent glycopolymer, inhibition



Cholera is a diarrheal disease caused by infection with Gram-negative bacterium *Vibrio cholerae*. It affects millions of people every year and is estimated to cause roughly 100 000 annual deaths worldwide.<sup>1</sup> Poor access to proper sanitation is believed to be the main reason that cholera persists, with the number of cases usually increasing dramatically during conflicts that disrupt access to clean drinking water.<sup>2–4</sup> The current gold standard treatment of severe cases consists of oral rehydration therapy with a complement of intravenous fluids. Antibiotics can also sometimes be used to help eliminate the infection.<sup>2,5</sup> Oral cholera vaccines with an efficacy of roughly 65% exist, but their efficacy is lower in children in endemic areas.<sup>6,7</sup> It is thought that unvaccinated populations in such endemic areas could greatly benefit from additional relatively low-cost treatments that ameliorate the disease symptoms and diminish the spread to family members during an outbreak.

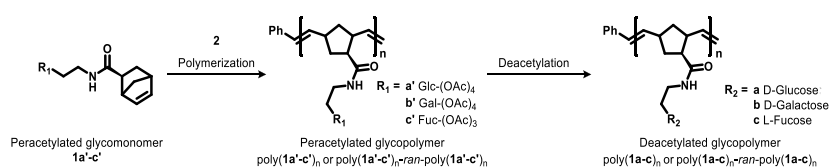
Cholera toxin (CT) is the main causative agent of cholera diarrhea. This is a holotoxin secreted by the bacterium upon colonization of the small intestine (SI). The toxin is composed of five binding B subunits (CTB) responsible for cellular uptake and one active subunit (CTA) that generates the

diarrheal symptoms.<sup>8</sup> For CT to intoxicate the host, CTB first binds to the small intestinal epithelium, resulting in cellular uptake and retrograde CTA transport to the endoplasmic reticulum. Following transport to the cytoplasm, CTA then covalently modifies the  $\alpha$ -subunit of the G protein  $G_s\alpha$  via ADP-ribosylation, leading to a constant cellular activated state of  $G_s\alpha$ . The consequence is increased production of intracellular cAMP and activation of protein kinase A, which in turn phosphorylates the cystic fibrosis transmembrane conductance regulator. This chloride ion channel then actively transports ions into the intestinal lumen, generating osmotic pressure and causing unabated secretion of water from SI epithelial cells (SI-ECs).

Received: January 9, 2020

Published: March 5, 2020



Scheme 1. Norborneyl Glycopolymers Prepared<sup>a</sup>

<sup>a</sup>Catalyst 2 is dichloro[1,3-bis(2,4,6-trimethylphenyl)-2-imidazolidinylidene](benzylidene)bis(3-bromopyridine)ruthenium(II). Abbreviations used in the text: poly(1a')<sub>100</sub>, pGlc<sub>100</sub>; poly(1b')<sub>100</sub>, pGal<sub>100</sub>; poly(1c')<sub>100</sub>, pFuc<sub>100</sub>; poly(1b')<sub>n</sub>-ran-poly(1c')<sub>n</sub>, pGal<sub>n</sub>Fuc<sub>n</sub>; poly(1a)<sub>100</sub>, Glc<sub>100</sub>; poly(1b)<sub>100</sub>, Gal<sub>100</sub>; poly(1c)<sub>100</sub>, Fuc<sub>100</sub>; and poly(1b)<sub>n</sub>-ran-poly(1c)<sub>n</sub>, Gal<sub>n</sub>Fuc<sub>n</sub>, where  $n = \text{DP}$ .

Each subunit of CTB has a binding site facing the CTA subunit distally. This site was shown almost 50 years ago to bind the GM1 glycosphingolipid with very high affinity.<sup>9–11</sup> Incorporating GM1 into membranes greatly increases the sensitivity of the cell to CT-mediated intoxication.<sup>12</sup> Consequently, GM1 has been described as the main ligand for CTB, and several inhibitors aimed at blocking this binding to the canonical site of CTB have been generated and reviewed extensively in Kumar and Turnbull.<sup>13</sup> Some of these carbohydrates that are mimics of GM1 could, in monovalent form, block CTB binding to GM1.<sup>14,15</sup> However, the multivalent display of these mimics or GM1 oligosaccharide (GM1-os) exhibited a greatly enhanced inhibitive capacity to CTB.<sup>16–20</sup> Indeed, this multimeric display of GM1 or GM1 mimics has also been shown to result in inhibition of the toxic effect of CT *in vivo* in mice and in human colonic cell lines and enteroids.<sup>19–21</sup>

However, the level of GM1 is extremely low in the human SI<sup>22</sup> and is also low in cell lines derived from the human colon that have often been used for the functional assessment of CT toxicity.<sup>22–26</sup> Human SI-ECs instead abundantly express fucosylated structures including histo-blood group antigens (HBGAs) that, albeit with lower affinity, bind to an additional site on CTB situated laterally and closer to the A subunit than the canonical site.<sup>27,28</sup> We have previously shown that occupying this noncanonical site with fucosylated HBGAs such as Le<sup>x</sup> or Le<sup>y</sup> or with polymers carrying fucose (Fuc) blocks CTB binding to primary human SI-ECs.<sup>29</sup> Furthermore, preincubating the primary human SI-ECs with a lectin that cross-links fucosylated glycans efficiently blocked subsequent CT-induced secretion.<sup>29</sup> Interestingly, a lectin that binds terminal galactose on human SI-ECs also inhibited the toxic effects of CT, although the same lectin showed no detectable block on CTB binding to SI-ECs, results that may point to an essential role for high-affinity Gal-terminated receptors such as GM1. Alternatively, the effects of the Gal-recognizing lectin could stem from its ability to cross-link structures on SI-ECs as well as the known toxicity of lectins applied at high concentrations.<sup>30</sup> The expression of HBGAs differs between individuals, and interestingly, the expression of only the smallest determinant, the unmodified H antigen with a terminal fucose, i.e., blood group O individuals, has been shown to be overrepresented among individuals with severe cholera symptoms. Interestingly, the differential capacity of CT to bind to a patient's variable levels of HBGAs via the noncanonical site has been suggested to be a potential underlying cause of disease severity.<sup>27</sup>

Inhibitors that could interfere with binding to galactosylated ligands (including GM1) via the CTB canonical site and simultaneously effect the binding to fucosylated ligands via the

noncanonical site would be an attractive approach. Polymers can display sugars multivalently, which increases the avidity of low-affinity interactions between sugars and CTB. A study has also recently shown that a multimeric mixed display of fucose and a galactoside also inhibits CTB binding to both GM1 and fucose in an ELISA without a major loss of blocking capacity compared to that of the homopolymers.<sup>31</sup> This suggests that dual-site inhibitors could be effective in situations where both galactosylated and fucosylated ligands are utilized for binding and subsequent intoxication. An assessment of the efficacy of inhibitors of CT can be done by blocking the binding of CTB to selected immobilized ligands in an ELISA or to the surface of immortalized cell lines and cells from human or experimental animal primary tissues. ELISAs offer high reproducibility and direct measurements of blocking the CTB binding to specific ligands, but even so, the glycan display on lipids or proteins will impact the CTB binding<sup>29</sup> and could influence the blocking assessment. Immortalized cell lines are easily accessible and have been used in most studies evaluating CTB inhibitors, but the cell surface glycosylation pattern is decided by multiple intracellular transferases that most often are significantly altered upon tumor transformation. Moreover, cell surface glycosylation patterns are host- and tissue-specific.<sup>32,33</sup> These latter points could greatly influence the assessment of the inhibitors capacity to block CT intoxication that can be done *in vitro* by measuring an increase in the intracellular levels of mediators such as cAMP, ion secretion assessed by alterations in resistance over monolayers/explants, or *in vivo* by intestinal fluid accumulation.

In this study, we have created polymers with either only Fuc to bind the noncanonical site, galactose (Gal) to bind the canonical site of CTB, or copolymers with a mix of Gal and Fuc aimed at binding both sites. We tested the ability of these polymers to block CTB binding to GM1 and fucosylated ligands as well as primary tissues from the SI of mice and humans as well as enteroids derived from the latter. Moreover, we assessed the efficacy of these polymers to block CT-induced ion secretion in the human enteroids and *in vivo* in mice. We show that polymers with only Fuc efficiently block the binding of CTB to human SI-ECs, while polymers with Gal have a limited capacity to inhibit. However, their specific capacity to block the binding to murine SI-ECs is the reverse. On the other hand, polymers carrying a mix of Gal and Fuc can efficiently inhibit CTB binding to human and murine SI-ECs as well as partially block CT-mediated intoxication *in vivo* in mice and in human enteroids. Furthermore, although preincubating the toxin with free GM1-os did not reduce the detected binding of CTB to human enteroids, it completely mitigated CT-induced ion secretion from the same cells.

Hence, our results suggest that the collective binding of CT to human SI-ECs is vastly dominated by the noncanonical site, whereas a small amount of binding to the canonical site is required and sufficient for CT intoxication. In addition, our finding highlights the importance of complementing CTB binding studies with functional intoxication studies in clinically relevant human cells.

## RESULTS

**Polymers with Fuc Block CTB Binding to Lewis Antigens but Not GM1.** In this study, we designed sugar polymers to target the canonical binding site of CTB, the noncanonical binding site of CTB, both, or neither. We generated polymers containing D-galactose (Gal<sub>100</sub>), L-fucose (Fuc<sub>100</sub>), D-galactose, and L-fucose (Gal<sub>50</sub>Fuc<sub>50</sub>) or D-glucose (Glc<sub>100</sub>), where Gal<sub>50</sub>Fuc<sub>50</sub> is a random copolymer. We then evaluated the capacity of these polymers to block the binding of CTB to defined sugar structures and cells as well as to block CT-mediated intoxication. Norbornene derivatives were chosen for their polymer backbone (Scheme 1). Norbornenes undergo ruthenium-catalyzed ring-opening metathesis polymerization with robust and effective control over molecular weight. The synthesis of sugar monomers from a racemic mixture of exo-5-norbornene-2-carboxylic acid and their preparation has been reported previously.<sup>34</sup> The molecular weights and dispersities of peracetylated glycopolymer precursors determined by gel permeation chromatography are presented in Table 1.

**Table 1. Molecular Weights of Polymers<sup>a</sup>**

| polymer   | M/C ratio <sup>b</sup> | $M_{\text{theor}}^b$ | $M_n^b$ | $M_w^b$ | $\bar{D}^b$ | DP <sup>b</sup> |
|---|------------------------|----------------------|---------|---------|-------------|-----------------|
| pGlc <sub>100</sub>                               | 100:1                  | 51 300               | 35 600  | 44 000  | 1.28        | 69              |
| pGal <sub>100</sub>                               | 100:1                  | 51 300               | 55 400  | 61 300  | 1.11        | 108             |
| pFuc <sub>100</sub>                               | 100:1                  | 45 500               | 59 500  | 66 300  | 1.12        | 131             |
| pGal <sub>5</sub> Fuc <sub>5</sub>                | 10:1                   | 4900                 | 7300    | 8200    | 1.12        | 15              |
| pGal <sub>15</sub> Fuc <sub>15</sub>              | 30:1                   | 14 600               | 15 500  | 18 100  | 1.17        | 30              |
| pGal <sub>50</sub> Fuc <sub>50</sub> <sup>c</sup> | 100:1                  | 48 400               | 54 800  | 62 800  | 1.15        | 113             |
|   |                        |                      | 55 800  | 66 500  | 1.19        | 115             |

<sup>a</sup>Polymers were analyzed using GPC with static light scattering (SLS) and refractive index (RI) detection in their protected peracetylated form prior to deprotection. Chromatogram traces are shown in Figures S1 and S2. <sup>b</sup>M/C ratio, 1a'-c' to catalyst 2 ratio;  $M_{\text{theor}}$ , theoretical molecular weight;  $M_n$ , number-average molecular weight;  $M_w$ , weight-average molecular weight;  $\bar{D}$ , dispersity; DP, degree of polymerization. <sup>c</sup>Two batches were prepared and characterized separately.

We next assessed the capacity of the different polymers to block the binding of CTB to GM1 or triLe<sup>x</sup> linked to proteins. GM1 and triLe<sup>x</sup> are known to bind to the canonical and noncanonical sites of CTB, respectively.<sup>27,35</sup> Therefore, ELISA plates were coated with GM1 or triLe<sup>x</sup> conjugated to human serum albumin (HSA). Then CTB-HRP preincubated with titrated amounts of the different sugar polymers were added to the ELISA plates. We found that both Fuc<sub>100</sub> and Gal<sub>50</sub>Fuc<sub>50</sub> readily blocked CTB binding to triLe<sup>x</sup>, with Gal<sub>50</sub>Fuc<sub>50</sub> showing the greatest efficacy (Figure 1A). Gal<sub>100</sub> had a limited effect and required much higher concentrations to block CTB binding to triLe<sup>x</sup> (Figure 1A). However, the blocking of CTB binding to GM1 was observed only with Gal<sub>100</sub>, and the blocking remained partial even at excess concentrations

(Figure 1B). Collectively these results show that the Gal<sub>50</sub>Fuc<sub>50</sub> has the highest capacity to bind CTB. Interestingly, Fuc<sub>100</sub> and Gal<sub>50</sub>Fuc<sub>50</sub> polymers block only the binding to HBGA via the noncanonical triLe<sup>x</sup> site and not to GM1 through the canonical site on CTB.

Next, we evaluated if the observed block was dependent on the sugar proximity and density within the polymers or if the effect of random copolymer Gal<sub>50</sub>Fuc<sub>50</sub> could be mimicked by blending Gal<sub>100</sub> and Fuc<sub>100</sub> (Figure 1A). A very small decrease in the blocking efficiency of CTB binding to triLe<sup>x</sup> was detected when using a blend of equimolar Gal<sub>100</sub> and Fuc<sub>100</sub> as compared to random copolymer Gal<sub>50</sub>Fuc<sub>50</sub> (Figure 1A). Only a small decrease in the signal was observed when blocking CTB binding to GM1 with the polymer blend compared to Gal<sub>50</sub>Fuc<sub>50</sub> (Figure 1B). To evaluate the impact of polymer length on CTB blocking, two shorter lengths were tested: Gal<sub>15</sub>Fuc<sub>15</sub> and Gal<sub>5</sub>Fuc<sub>5</sub>. As shown in Figure 1C, the shorter polymers had severely reduced blocking efficacies of CTB binding to triLe<sup>x</sup> compared to Gal<sub>50</sub>Fuc<sub>50</sub> (Figure 1A,C). Moreover, and in line with previous experiments (Figure 1B), no GalFuc polymers of any length had any inhibitory effect on CTB binding to GM1 (Figure 1D). We did not test any polymers longer than 100 sugars because for this type of polymer decreased solubility is observed with increasing length.

Collectively, these experiments show that fucose-containing polymers specifically block the binding of HBGA ligands to CTB, while galactose polymers confer limited blocking of CTB binding to GM1. Furthermore, shorter versions of the GalFuc polymers are less effective blockers, but a blend of Gal<sub>100</sub> and Fuc<sub>100</sub> polymers is as potent as the Gal<sub>50</sub>Fuc<sub>50</sub> copolymer in blocking the CTB binding to only HBGA.

**Polymers with Gal but Not with Fuc Block the CTB-Binding Murine Cells.** To assess the capacity and site specificity of the polymer-mediated blocking of CTB-binding to live cells, single cell suspensions of murine SI-ECs and mesenteric lymph nodes (MLNs) were generated. The cells were stained with CTB-biotin preincubated with the different polymers. Then, levels of CTB binding to the cells were assessed using flow cytometric techniques (Figures S3 and S4). As expected, CTB did not bind to the KO lymphocytes from the MLNs, confirming that GM1 or GM1-related glycolipids account for all CTB binding to murine lymphocytes (Figure S5).<sup>29</sup> Furthermore and as previously published, we observed that CTB still bound to SI-ECs from the KO, albeit to a lower extent (Figure 2A).<sup>29</sup> However, Gal<sub>100</sub> blocked CTB binding to WT SI-ECs and lymphocytes with the same efficacy as the Gal<sub>50</sub>Fuc<sub>50</sub> copolymer (Figures 2B and S5). In contrast, Fuc<sub>100</sub> has very little blocking effect on WT SI-ECs (Figure 2A,B) and lymphocytes (Figure S5). Moreover, the blocking pattern of CTB binding to KO SI-ECs by the polymers was similar to that observed with WT SI-ECs, albeit slightly reduced (Figure 2C). This suggests that the canonical site is the sole determinate of CTB binding to murine cells. This result is also in line with our previously published data showing that the binding of CTB to these cells is independent of fucosylated receptors.<sup>29</sup>

**Gal<sub>50</sub>Fuc<sub>50</sub> Polymers Block CT-Induced Fluid Accumulation in Mouse SI.** Next, we wanted to assess if Gal<sub>50</sub>Fuc<sub>50</sub> could interfere with intoxication caused by CT. Hence, murine ligated loops of the proximal SI were made and injected with CT that had been preincubated with or without the Gal<sub>50</sub>Fuc<sub>50</sub> polymer. Four hours later, the mice were

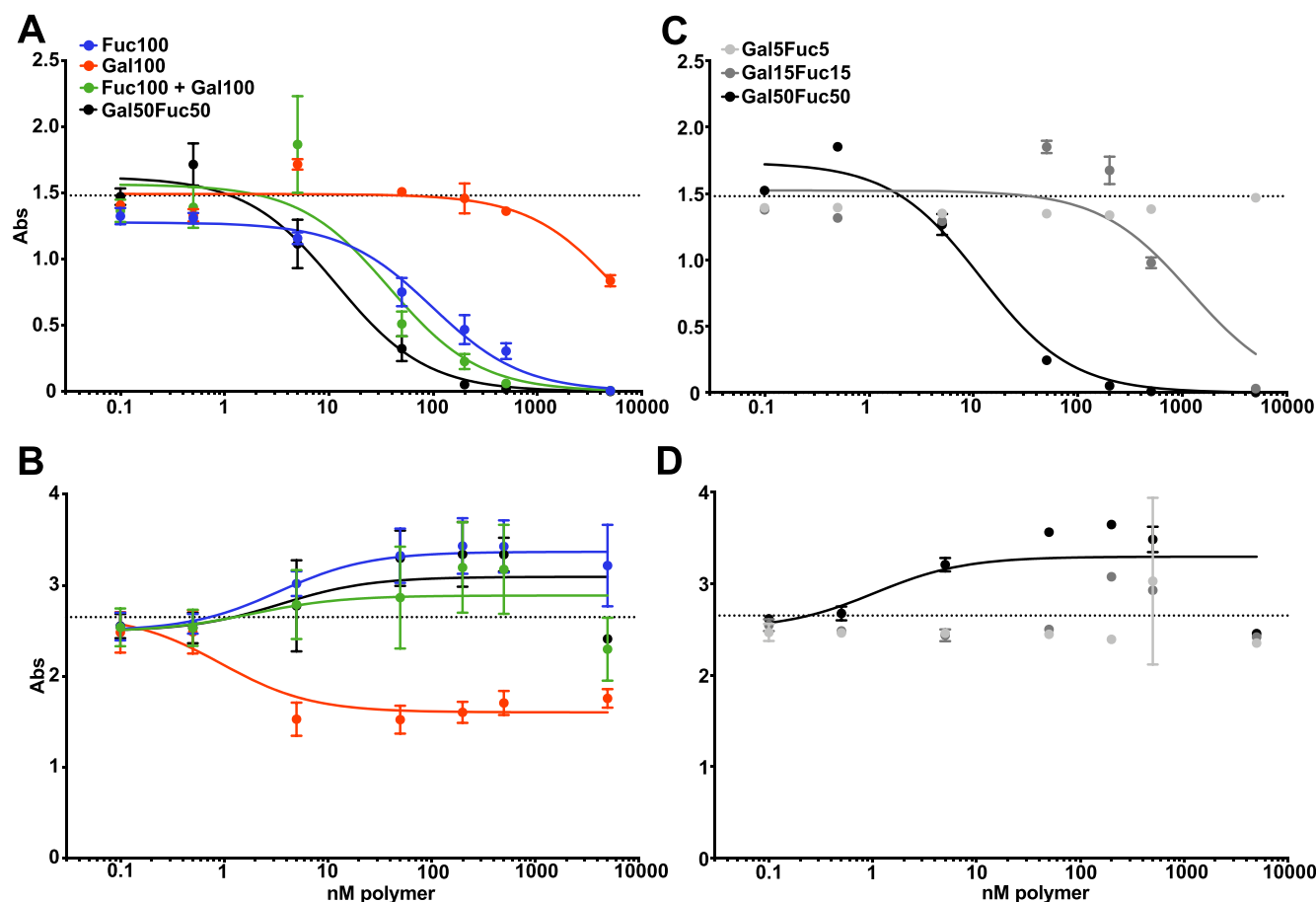


**Figure 1.** Polymer block in ELISA of CTB binding to triLe<sup>x</sup> and GM1. (A and C) Plates were coated with triLe<sup>x</sup>-HSA and probed with CTB preincubated with the different polymers. (B and D) Plates were coated with GM1-HSA and probed with CTB preincubated with the different polymers. In (A) and (B), all polymers used displayed 100 sugars. In (C) and (D), the length of the copolymer varies with the number of displayed sugars. Curve fits were made using a three-parameter fit to eq 1. Dotted lines indicate unblocked CTB binding. Graphs show a representative experiment out of three independent experiments, and error bars are the SD of intra-assay duplicates or quadruplicates.

sacrificed, and the loops were weighed and their lengths were recorded.<sup>36–38</sup> We visually detected a partial polymer-mediated block of CT-induced fluid accumulation in the loops (Figure 2D). Furthermore, this effect was statistically significant when assessed in multiple animals where the weight/length of intestine was measured to account for the difference in size of the mice (Figure 2E). In conclusion, the galactose-containing polymers efficiently block the binding of CTB to both WT murine lymphocytes and primary SI-ECs, while the Fuc<sub>100</sub> polymer has a very limited effect. Moreover, the preincubation of CT with the Gal<sub>50</sub>Fuc<sub>50</sub> copolymer partially blocks the toxin-induced fluid accumulation in vivo.

**Gal<sub>50</sub>Fuc<sub>50</sub> is a Potent Blocker of CTB Binding to Human SI-ECs.** Having shown that the Gal<sub>50</sub>Fuc<sub>50</sub> random copolymer has the potential to block CT-mediated intoxication in mice (Figure 2), we next tested the capacity of these polymers to block CTB binding to isolated human primary SI-ECs as assessed by flow cytometry (Figure S6). In line with our previously published data<sup>22,28</sup> and in contrast to what we observed in the murine intestine (Figure 2), CTB binding to human SI-ECs was almost completely blocked by preincubation with the Fuc<sub>100</sub> polymer, whereas the Gal<sub>100</sub> polymer displayed only a partial blocking effect (Figure 3A,B). Moreover, the Gal<sub>50</sub>Fuc<sub>50</sub> polymer was more than 10 times more efficient at blocking CTB binding to human SI-ECs than

the Fuc<sub>100</sub> polymer (Figure 3B). In contrast, the Glc<sub>100</sub> polymer showed no blocking effect, confirming that also with human primary tissues the blocking observed is sugar-dependent and not an unspecific polymer effect (Figure 3B).

We next assessed if polymer length was important for blocking CTB binding in a situation where the fucose-dependent binding is considerable. Gal<sub>3</sub>Fuc<sub>5</sub> and Gal<sub>15</sub>Fuc<sub>15</sub> polymers were tested and compared to Gal<sub>50</sub>Fuc<sub>50</sub>. We observed a marked decrease in blocking efficacy when shortening the polymers both in terms of equimolar amounts of polymer and when normalizing to the number of polymer-attached sugars (Figure 3B,C). When comparing equimolar amounts of polymer-attached sugars, the Gal<sub>50</sub>Fuc<sub>50</sub> polymer was roughly 3 times more potent than Gal<sub>15</sub>Fuc<sub>15</sub> and 175 times more potent than Gal<sub>3</sub>Fuc<sub>5</sub> polymers.

Heat-labile toxin (LT) secreted by ETEC shows very high similarity to CTB and has been shown to bind GM1. However, additional glycoconjugate ligands have been described.<sup>39–41</sup> We therefore assessed, on a small subset of donors, the capacity of the Gal<sub>50</sub>Fuc<sub>50</sub> polymer to block LTB binding to SI-ECs. We observed the same pattern of polymer blocking as for CTB, although the SI-ECs tended to bind more LTB than CTB (Figure 3D,E), indicating that the Gal<sub>50</sub>Fuc<sub>50</sub> polymer is relevant not only for blocking CT binding but also for blocking LT binding to the human SI. In conclusion, we show that



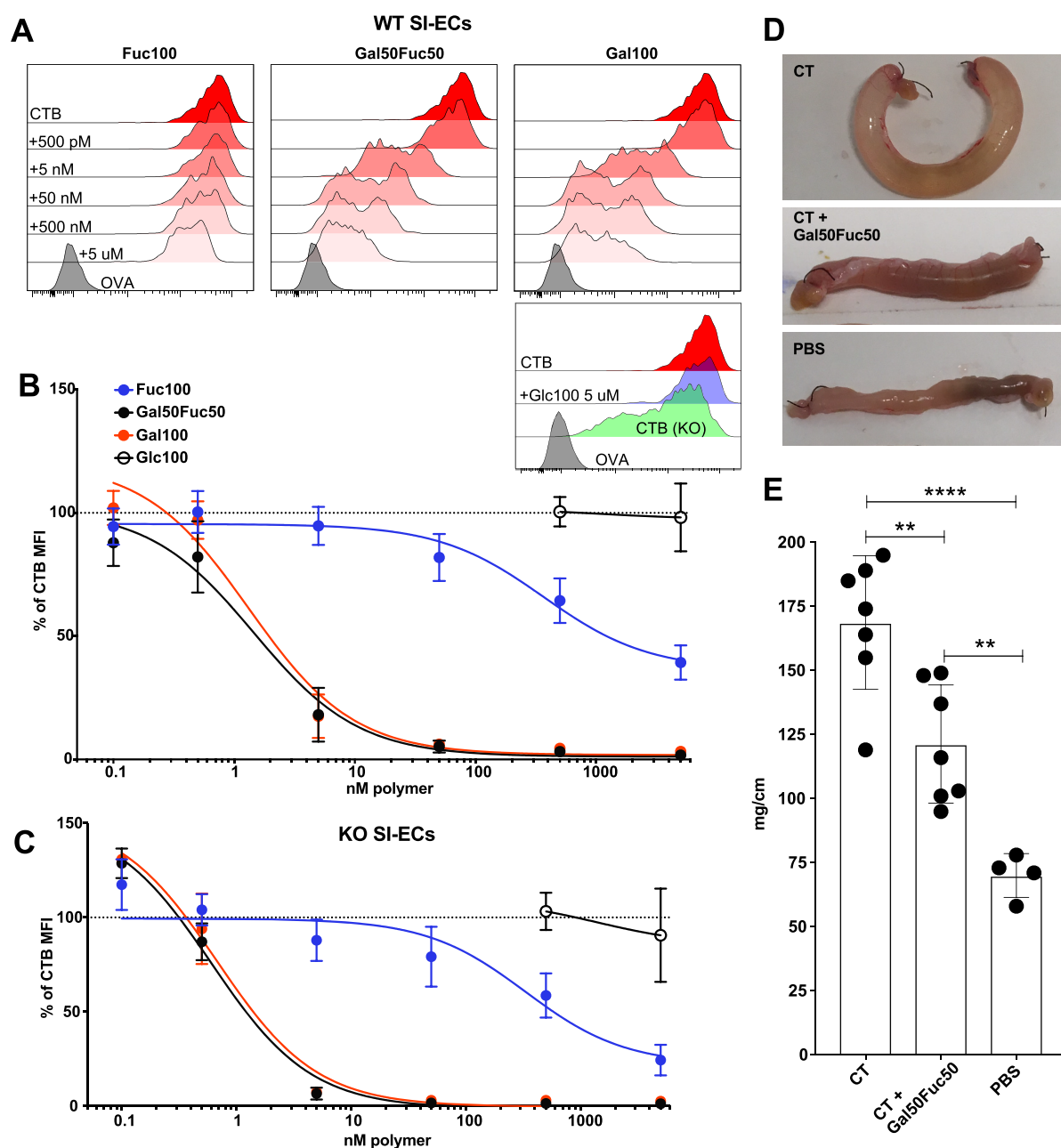


**Figure 2.** Evaluation of glycopolymers' capacity to block CTB binding to murine SI enterocytes and intoxication. (A–C) Cells were isolated from murine SI, stained for common cell markers and with CTB to analyze the polymer block by flow cytometry. Full gating can be seen in Figure S4. Panel (A) shows representative histograms of CTB binding to WT EpCAM<sup>+</sup> cells with or without the polymer block. Panels (B) and (C) show graphs of gMFI for CTB binding after the polymer block. The values are normalized to the % of unblocked CTB gMFI. Data is pooled from three independent experiments with two to three mice in each experiment, and error bars represent the SD. (D) Representative pictures of ligated loops after 4 h of CT (10  $\mu$ g/mL) treatment with or without Gal<sub>50</sub>Fuc<sub>50</sub> polymer (40  $\mu$ M) or just PBS *in vivo*. (E) Bar graph showing fluid accumulation as the length/weight ratio of the ligated loops. In each animal, two loops were created. Statistics were calculated using one-way ANOVA with Tukey correction. Two stars represent  $p < 0.01$ , and four stars represent  $p < 0.001$ . Error bars represent the SD, and each dot represents a loop.

fuco-se-containing polymers can efficiently block the binding of CTB and LTB to primary human SI-ECs. The Gal<sub>50</sub>Fuc<sub>50</sub> polymer has greater blocking efficacy, although the Gal<sub>100</sub> polymer still mediates the partial blocking of CTB binding at high concentrations. These results indicate that both the canonical and noncanonical sites are of importance when generating reagents aimed at blocking the binding of CT to human SI-ECs and subsequent intoxication.

**CT Intoxication of Human Enteroids Is Partially Blocked by Gal<sub>50</sub>Fuc<sub>50</sub> and Completely Inhibited by GM1.** Finally, to functionally assess the capacity of polymers to block the intoxication of human SI, we chose to establish human SI enteroid cultures, as the great similarity between primary tissue and enteroid cultures has previously been described.<sup>42</sup> Crypts were isolated from human jejunum tissue and cultured in cell culture medium promoting Lgr5<sup>+</sup> stem cell regeneration. These enteroid cultures were then differentiated

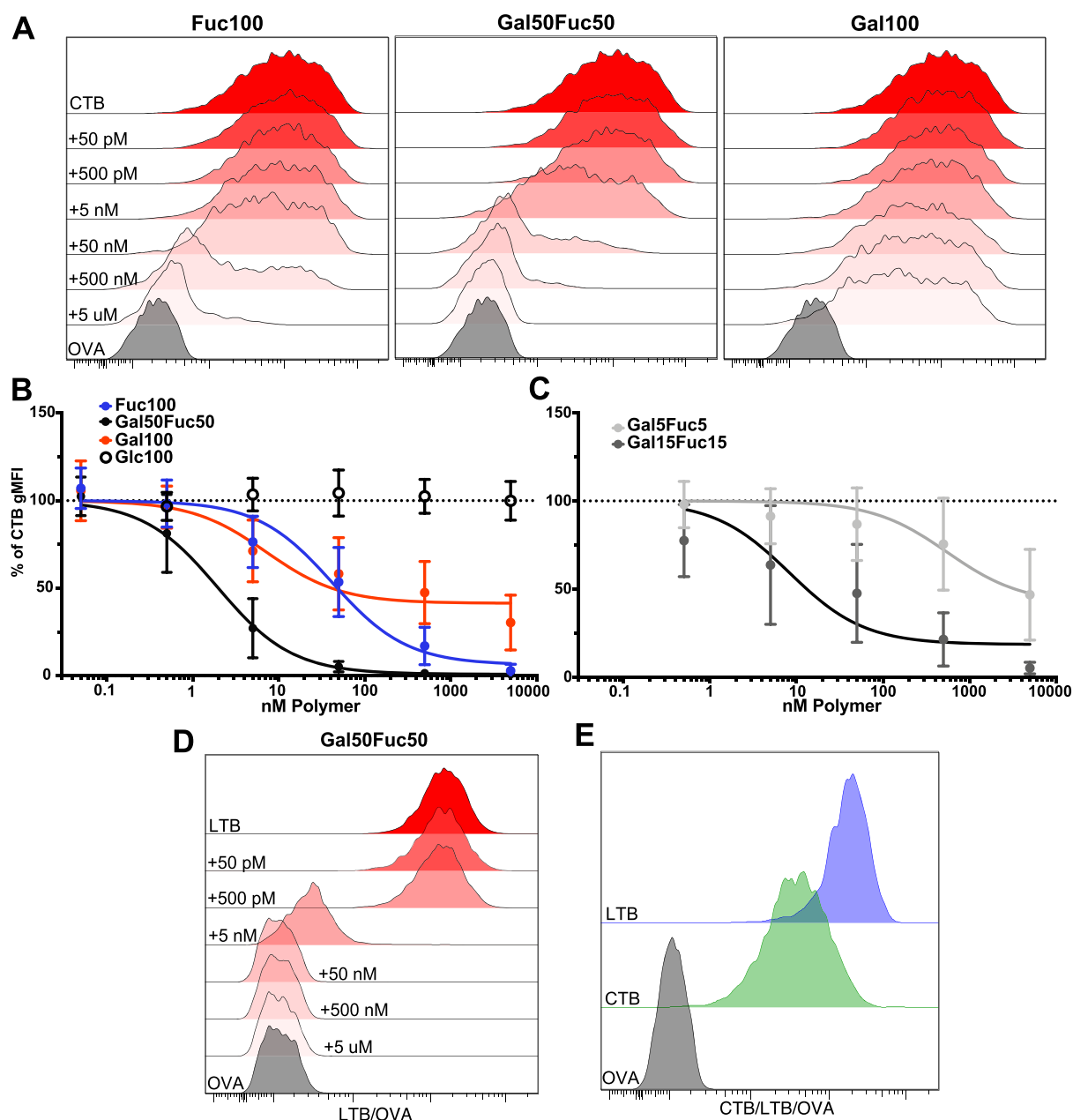


**Figure 3.** Flow cytometry evaluation of glycopolymers' capacity to block CTB and LTB binding in human SI enterocytes. Cells were isolated from human SI and stained for common cell markers and with CTB to analyze the polymer block by flow cytometry. Full gating can be seen in Figure S6. Panel (A) shows representative histograms of CTB binding to EpCAM+ cells with or without a polymer block. Panels (B) and (C) show graphs of gMFI for CTB binding after long polymer (B) and short polymer (C) blocks ( $n = 5-10$  donors). (D) Representative (out of five donors) histogram of LTB binding to EpCAM+ cells with or without a polymer block. (E) Representative (out of five donors) histogram of CTB and LTB binding to EpCAM+ cells. The values are normalized to the % of unblocked CTB gMFI. Error bars represent the SD.

by removing growth factors for stem cells (Figure 4A), resulting in the appearance of the mature cell types present in the human small intestine such as mucus-producing cells, enterocytes with microvilli, and lysozyme-producing cells (Figure 4B–D).

We then performed flow cytometry assessments of CTB binding (following preincubation with polymers) to differentiated enteroid cells from four different donors (Figures S7 and 4E,F). We observed that the differential capacity of the polymers to block CTB binding to enteroid cells reproduced the results obtained with primary human SI-ECs (Figure 3), with the copolymer being most efficient, followed by the Fuc<sub>100</sub>

and Gal<sub>100</sub> polymers (Figure 4E,F). We have previously shown that preincubating CTB with GM1-os has a limited capacity to block the binding of CTB to primary human SI-ECs and with significant variability between donors.<sup>29</sup> Consistent with our previous work, GM1-os showed a very limited, if any, capacity to block CTB binding to four human enteroid cultures compared to the copolymer (Figure 4F). The ABO status and potential variable expression of HBGAs of these established cultures have not yet been determined.

To evaluate if the polymers block CT-induced ion efflux (intoxication), the enteroid cells were then seeded into permeable trans-well inserts, allowing for transmembrane

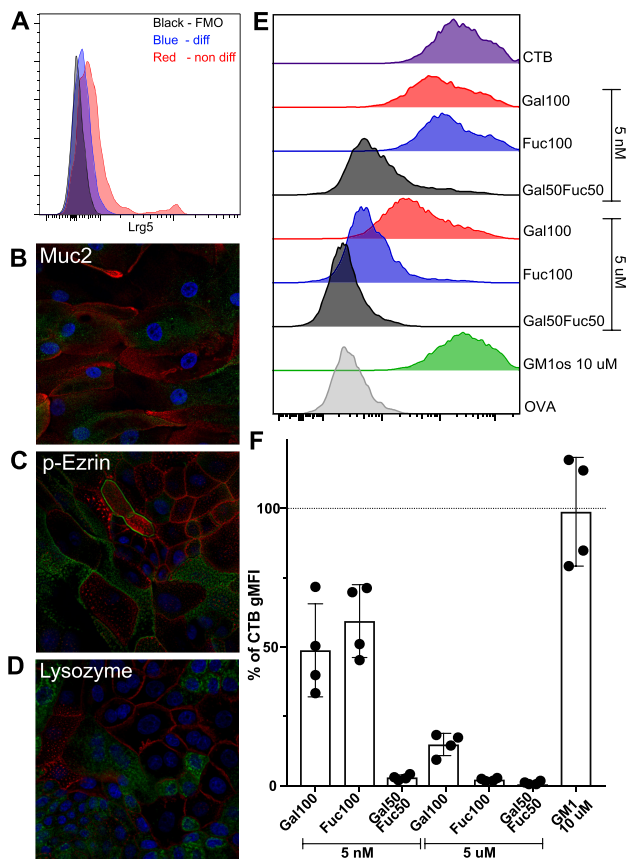


**Figure 4.** Enteroid characterization and functional evaluation of the polymer block. (A) Enteroid cells were evaluated using flow cytometry for the presence of Lrg5<sup>+</sup> stem cells. (B–D) Enteroid cells were cultured on a transwell insert and differentiated into a non-stem-cell state for 5 days. For all panels, the DAPI stain is blue and the enterocyte marker phalloidin stain is red (for cell visualization). Markers were used to identify different cell types (green) such as goblet cells (B), mature enterocytes (C), and Paneth cells (D). (E) One representative histogram out of two independent experiments of polymer and the GM1-os block of CTB binding to enteroid cells (flow cytometry). Full gating can be seen in Figure S7. One representative analysis out of four donors. (F) Bar graph showing the % of CTB gMFI on cells from four different donors after preincubating CTB with GM1-os or polymers. Error bars are SD.

voltage and resistance measurements. Out of the four enteroid cultures, only one grew to a high level of confluency required for reliable and consistent measurements. For these experiments, the enteroids were differentiated for 5 days prior to apical challenge with CT preincubated with or without our polymers or GM1-os. Then the voltage and resistance were measured using an ohm meter. These measurements were used to calculate the short circuit current ( $I_{sc}$ ) per  $\text{cm}^2$  where the values were normalized to the PBS control for each time point. We observed a CT-dependent effect after 3 h, which lasted throughout the experiment (Figure 5). Preincubating CT with either the Fuc<sub>100</sub> or Glc<sub>100</sub> polymers resulted in no blocking effect compared to untreated CT (Figure 5), while CT treated with the Gal<sub>100</sub> polymer showed a delayed and minor reduction in response (Figure 5). Furthermore, a partial and sustained block of CT by the Gal<sub>50</sub>Fuc<sub>50</sub> polymer was observed (Figure 5), although the same concentration of Gal<sub>50</sub>Fuc<sub>50</sub> completely blocked all detectable CTB binding when measured by flow

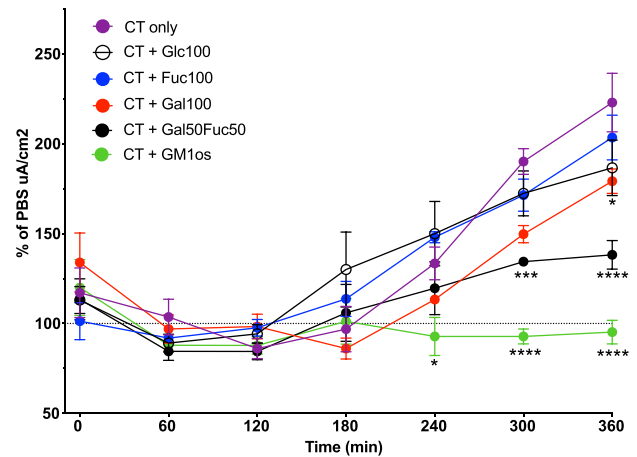


**Figure 5.** CT challenge of enteroid cells. Differentiated enteroid cells were used to evaluate the polymer (5  $\mu\text{M}$ ) block of CT (0.1  $\mu\text{g}/\text{mL}$ ) intoxication. The graph shows  $I_{sc}$  values pooled from four independent experiments using enteroids from one donor. Values are normalized to PBS-treated control cells at each time point. Statistics calculated using two-way ANOVA with Tukey correction in Prism software. \*Represents a significant difference between the closest data point and CT only. One star represents  $p < 0.05$ , three stars represent  $p < 0.001$ , and four stars represent  $p < 0.0001$ . Error bars are the SEM.

cytometry (Figure 4E,F). In contrast, the preincubation of CT with GM1-os completely blocked all CT-mediated ion secretion, while using the same concentration of GM1-os had only a minor effect on CTB binding to enteroids derived from the same donor (Figures 4E,F and 5). Collectively, these results show that aggregating CT with the Gal<sub>50</sub>Fuc<sub>50</sub> polymer effectively blocks binding to human SI-EC and significantly reduces the intoxication of these cells. Interestingly, preincubating the toxin with GM1-os has a limited effect on the total binding detected for CTB to SI-ECs but completely inhibits the secretory response to the holotoxin.

## DISCUSSION

Improved vaccines against enterotoxin producing bacteria as well as complementary strategies to reduce the spread of disease during outbreaks are needed. Hence, here we show that norbornene polymers carrying a mix of Fuc and Gal can effectively block CTB and LTxB binding to primary human SI-ECs. These polymers also partially inhibit the CT-mediated intoxication of human SI enteroids as well as CT-induced fluid accumulation in murine SI. Using our monosugar polymers, we found that the largely fucose-dependent but galactose-independent binding of CTB to human SI-ECs is different from that of the fucose-independent but galactose-dependent binding of CTB to murine SI-ECs. Moreover, although the effect of occupying the canonical site with the high-affinity-ligand GM1 had only a minor effect on the total binding of CTB to human SI-EC, this treatment completely inhibits CT-mediated ion secretion by human SI enteroids.

The polymer-induced aggregation of enterotoxins could be an effective and relatively low cost therapeutic since the polymer-toxin complexes have no theoretical size limit and thus readily become too large for intestinal cellular uptake. This is an effect that cannot be produced by free sugars or oligosaccharides that occupy only one binding site per molecule. It has not previously been shown that a fucose-

and galactose-containing polymer can inhibit CT intoxication in human enteroids or in mice. Our results indicate that using a mixed sugar polymer has an advantage over inhibitory molecules targeting only one of the two sites on CTB. A recent study has shown that a mixed polymer with fucose and a galactoside can block the binding of CTB to both GM1 and fucosylated structures.<sup>31</sup> However, our study extends this finding as we show the necessity of complementing the blocking of CTB-binding studies to ligands and even to primary cells, with functional blocking studies of CT-induced intoxication when assessing the efficacy of the inhibitors of CT. The model of confluent monolayers cultured from human intestinal enteroids combined with the measurement of changes in resistance as the assessment of ion transport offers a unique possibility to measure CT induced in secretion in a donor-selective fashion. We show a partial blocking of CT intoxication by the Gal<sub>50</sub>Fuc<sub>50</sub> polymer and a complete inhibition of toxicity by GM1-os, although the latter hardly blocks binding to the intestinal enteroids. This pinpoints that the level of binding of CT via the canonical site to SI-EC is virtually undetectable to human intestinal cells due to the extensive presence of fucosylated structures that bind CTB via the noncanonical site. A complete block of CT-induced intoxication by GM1 or GM1-based inhibitors has recently been shown in 3-D cultures of colonic human enteroids and also in mice.<sup>19–21</sup> However, the evaluation of the influence of CT binding to fucosylated ligands on the apical surface of human SI-ECs was not possible in 3-D enteroid cultures as the apical surface is facing inward and is thus not exposed to CT. In addition, we have previously shown and confirm in this study that the level of binding of CTB to fucosylated structures in mice via the noncanonical site is very limited.

We found that the random copolymer Gal<sub>50</sub>Fuc<sub>50</sub> was unable to block the binding of CTB to HSA-linked GM1 in ELISA. However, CTB binding to primary human SI-ECs and enteroids was blocked with either the copolymer or Fuc homopolymer, even at low concentrations. The Gal homopolymer at higher concentrations also partially blocked binding. In contrast, the binding of CTB to murine SI-ECs that occurs in the complete absence of GM1 in the  $\beta$ 4GalNAcT KO mice was blocked by the Gal<sub>50</sub>Fuc<sub>50</sub> and Gal<sub>100</sub> polymers, while the Fuc<sub>100</sub> polymer had a limited effect. This indicates that CTB binds to galactosylated ligands remaining on SI-EC in KO mice. Furthermore, CTB binding to murine lymphocytes was also inefficiently blocked by the Fuc<sub>100</sub> polymer, indicating that galactose-containing CTB receptors are also present on these cells. These receptors should therefore be GM1 or GM1-related glycosphingolipids (GSLs), as no binding of CTB to murine T or B cells can be observed in  $\beta$ 4GalNAcT KO mice. However, the main receptor on murine T cells is most likely not GM1 but rather other GM1-related GSLs with lower affinity for CTB as Gal<sub>50</sub>Fuc<sub>50</sub> polymers readily blocked CTB binding to murine T cells.

We and others have previously shown that CT can induce cAMP production in cells devoid of GM1 and that this is partially due to fucosylated glycoconjugates.<sup>29,43,44</sup> However, our Fuc<sub>100</sub> polymer showed no effect in limiting the CT-mediated intoxication of human enteroids but instead the copolymer Gal<sub>50</sub>Fuc<sub>50</sub> partially inhibited CT-mediated intoxication. We have also previously shown that the fucose-binding lectin AAL completely blocks the CT-induced ion secretion in fresh human jejunal tissue.<sup>29</sup> Hence, it was somewhat unexpected that Fuc<sub>100</sub> did not block CT intoxication.

However, the AAL lectin has a high affinity for fucose and has a very low off-rate for some of its ligands.<sup>45</sup> The polymer, on the other hand, has several CTB interactions, but all have low affinity. The capacity of GM1-os preincubated with CT to inhibit the CT-mediated intoxication of human enteroids indicates a complete dependence on the canonical site and galactosylated receptors for internalization and subsequent unabated ion secretion. This confirms our previous findings with primary human SI tissues, where pretreating with the galactose-binding lectin PNA did not result in a noticeable block of CTB binding but efficiently blocked CT-mediated intoxication.<sup>29</sup>

Our results using primary human SI-ECs support a theory that CT uses the noncanonical site to first bind to a primary glycoprotein receptor with low affinity. After that, and if present on the cell, GM1, GM1-related GSL, or other receptors with terminal galactose will outcompete the low-affinity fucosylated receptor or bind simultaneously as suggested by others.<sup>46</sup> Then, following stable binding through the canonical site, CT is internalized. Since CT would be concentrated close to the cell membrane by the primary receptors, this could facilitate uptake by receptors that are close to the membrane, such as GM1. This model could also help to explain why humans, in contrast to mice, express fucosylated HBGA structures that can bind CTB and are dramatically more sensitive than mice to CT intoxication. However, if the fucosylated HBGAs were obligatory facilitators of subsequent galactosylated receptor-dependent intoxication, it would be expected that the Fuc<sub>100</sub> polymer should have influenced CT-mediated intoxication of the human enteroids. Despite this, no reduction in toxicity was observed in the enteroid monolayer established from one donor when preincubating CT with saturating concentrations of Fuc<sub>100</sub> indicating that binding via the noncanonical site plays no major role in facilitating CT intoxication. Importantly, the expression of fucosylated HBGAs varies between individuals and has been suggested to be linked to the great difference in severity of disease symptoms among infected individuals.<sup>2,47–50</sup> Hence, in order to determine if fucosylated structures are facilitators of subsequent intoxication and if so to which extent, a library of enteroids from humans with characterized HBGA expression needs to be generated. Furthermore, this assessment needs to be functional as our results clearly show that the binding of CTB to the cells does not necessarily correlate with CT-mediated intoxication.

## ■ CONCLUSIONS

To summarize, we show that random copolymers carrying galactose and fucose can efficiently aggregate CTB, thereby blocking CTB binding to human enteroids as well as partially inhibiting CT-mediated intoxication in human enteroids and mice. Our results also suggest that although the collective binding of CT to human SI-ECs is vastly dominated by low-affinity interactions between the noncanonical site and fucosylated structures, it is the CTB binding by the canonical site to the comparatively few structures on the SI-ECs that is required for intoxication. This suggests that although the aggregation of CT with the Gal<sub>50</sub>Fuc<sub>50</sub> polymer is effective and partially blocks intoxication, in order for complete blocking the affinity of the interaction between the galactose on the polymer and the canonical site of CT needs to be increased. Otherwise, the natural ligand(s) on the SI-ECs with higher affinity for the canonical site will outcompete the polymer-bound galactose



and thereby cause the uptake of CT. Whether the high-affinity CTB binding ligand in the human intestine is solely the very scarcely expressed GM1 or other related galactose structures and if binding via the canonical site of CTB is facilitated by differentially expressed HBGAs remain to be determined.

## MATERIALS AND METHODS

### Polymer Preparation. General Polymerization Method.<sup>1</sup>

Grubbs third-generation catalyst was prepared as described in the literature.<sup>51</sup> To a vial containing dichloro[1,3-bis(2,4,6-trimethylphenyl)-2-imidazolidinyliidene](benzylidene)bis(3-bromopyridine)ruthenium(II) (**2**) under Ar was added anhydrous CH<sub>2</sub>Cl<sub>2</sub>. The desired volume with respect to the targeted polymer DP of catalyst **2** stock solution (1.0 mM) in anhydrous CH<sub>2</sub>Cl<sub>2</sub>, was transferred into a vial charged with Ar. The solution was chilled to 0 °C, the desired volume of peracetylated glycomonomer (**1a'**, **1b'**, **1c'**) solution from a CH<sub>2</sub>Cl<sub>2</sub> stock was added, and the solution was stirred for 3 h. The solution immediately turned light brown upon addition of monomers. The reaction was quenched with 100 μL of ethyl vinyl ether, and the solution was stirred for 10 min. The reaction mixture was directly precipitated into cold diethyl ether to obtain gray precipitate. Repeated precipitations were performed to improve the purity of the polymer. The resulting peracetylated glycopolymer was dried in vacuo and analyzed by GPC and <sup>1</sup>H NMR spectroscopy. The level of residual ruthenium catalyst was tested using ICP-MS and determined to be less than 0.4 ppm.

**General Deacetylation Procedure.**<sup>1</sup> To a vial charged with peracetylated polymer (52.4 mg) and K<sub>2</sub>CO<sub>3</sub> (107.5 mg) a 1:2 v/v mixture of THF/MeOH (8 mL) was added and the mixture was stirred for 2 h. To the vial was added 4 mL of H<sub>2</sub>O, and the mixture was allowed to stir for an additional 1 h. The solution was acidified with a 1:1 mixture of 1 M HCl/THF and concentrated in vacuo. The deacetylated polymer solution was further purified by dialysis using a commercially available dialysis membrane (MWCO 3500) against distilled deionized H<sub>2</sub>O for 72 h with H<sub>2</sub>O replaced every 8 h to ensure the complete removal of inorganic salts and leftover monomers. The dialyzed solution was lyophilized to obtain deacetylated polymer as a white solid (24.9 mg). Complete deacetylation and the absence of small organic molecules were confirmed by <sup>1</sup>H NMR spectroscopy. In the absence of nonsolvent impurities, we estimated the purity to be >95%.

**Polymer Characterization.** Gel permeation chromatography was performed with a GPC system composed of a Shimadzu SCL-10A controller, a Shimadzu LC-20AT pump, and a Shimadzu CTO-10AS column oven equipped with either a Phenomenex Phenogel 5 μm 10E4A, LC column 300 × 7.8 mm<sup>2</sup> or a Phenogel 5 μm Linear(2), LC column 300 × 7.8 mm<sup>2</sup>, a Brookhaven Instruments BI-DNDC refractometer, and a BI-MwA multiangle laser light scattering (MALLS) detector. HPLC-grade tetrahydrofuran was filtered through 0.45 μm nylon filter and used as the eluent with a flow rate of 0.7 mL/min at 30 °C. GPC chromatograms were calibrated using polystyrene standard calibration kits. The molecular weights and dispersities of peracetylated glycopolymers were calculated on the basis of the refractive index and light-scattering signals. Molecular weights of deacetylated glycopolymers (Glc<sub>100</sub>, Gal<sub>100</sub>, Fuc<sub>100</sub>, and Gal<sub>50</sub>Fuc<sub>50</sub>) were calculated by assuming complete deacetylation as confirmed via <sup>1</sup>H NMR spectroscopy and based on the molar mass of acetates with respect to DP.

**Bioassay Reagents.** Recombinant CTB (PDB ID SELD) and LTB were produced in-house.<sup>52</sup> CTB, LTb, and OVA were conjugated to biotin and/or HRP as previously described.<sup>29</sup> Active CT produced in *V. cholerae* was purchased from List Biological Laboratories, azide-free in powder form (product no. 100B). HSA-linked tri-Le<sup>x</sup> and GM1 (product no. 61/56 and 61/69, IsoSep) were used to coat ELISA plates for CTB binding. GM1 oligosaccharide was purchased from Elicityl (product no. GLY096).

Krebs ringer solution was prepared by mixing the following ingredients with distilled water: 118 mM NaCl, 4.69 mM KCl, 2.52 mM CaCl<sub>2</sub>, 1.16 mM MgSO<sub>4</sub>, 1.01 mM NaH<sub>2</sub>PO<sub>4</sub>, 25 mM NaHCO<sub>3</sub>, and 12.2 mM D-glucose. R10 medium was prepared from the following ingredients: RPMI1640 with 10 mM HEPES, 10% FBS, 2 mM L-glutamine, 1 mM Na-pyruvate, 1% PenStrep, and 10 μg/mL gentamicin (Gibco, Fisher Scientific).

**ELISA.** ELISA was performed using HSA-linked oligosaccharides (tri-Le<sup>x</sup> and GM1) which were immobilized in 96-well microplates at RT overnight (MICROLON 600 High Binding, Greiner, VWR) and subsequently blocked with 0.2% BSA (Sigma-Aldrich) in PBS at 37 °C. The plates were incubated with CTB-linked to HRP (conjugated using the Lightning-Link HRP Kit, Expedeon) with or without polymers in PBS + 0.2% BSA and 0.1% Tween20 (Sigma-Aldrich) at RT. To detect CTB-HRP binding, we used *o*-phenylenediamine dihydrochloride (OPD, Sigma-Aldrich, 1 mg/mL) dissolved in 0.1 M citrated buffer at pH 4.5 for 15 min, after which the reaction was stopped with H<sub>2</sub>SO<sub>4</sub>. To evaluate the absorbance, we used Lx800 (BioTek). Background values (absorbance in wells coated only with BSA but probed with CTB-HRP) were subtracted before graphing the data.

**Equation 1.** IC<sub>50</sub> was calculated using GraphPad Prism 7 with “Dose-response - Inhibition, log (inhibitor) vs response (three parameters)”. More information can be found at [graphpad.com/guides/prism/7](http://graphpad.com/guides/prism/7).

**Mice.** Mice  $-/-$  or  $+/-$  for the  $\beta$ 4GalNAcT-gene (C57BL/6 background) were kindly donated by Professor Ronald L. Schnaar (Johns Hopkins University School of Medicine, Baltimore, MD, USA). The  $-/-$  (KO) mice are deficient in complex (and most noncomplex) GSLs, as confirmed previously.<sup>53,54</sup> The mice were bred using heterozygous breeding and maintained in individually ventilated cages in the animal facility at Sahlgrenska Academy, University of Gothenburg, Sweden.  $+/-$  mice express similar levels of GM1 as  $+/+$  mice and were therefore used as WT together with normal C57BL/6 mice.<sup>55</sup> All animal experiments were performed in accordance with approved ethical permits granted by the regional animal ethics committee (ethics nos. 150/15 and 1092/17).

The jejunal section from mouse intestine (both WT and KO) was excised along with the mesenteric lymph nodes (MLN). The enterocytes were isolated using the same protocol as seen below for human intestine but without initial removal of the muscular tissue. The intestinal cells were stained with mAbs against CD45.2-FITC, EpCAM-APC-Cy7, CTB, OVA-biotin + SA-BV421, and live/dead marker Zombie Red to evaluate CTB binding to epithelial cells.

MLN cells were isolated by gently mashing the nodes through a 100 μm mesh filter. The cells were stained with mAbs against CD3-APC and B220-FITC and with CTB or OVA-biotin, followed by streptavidin-BV421 and live/dead marker Zombie Red to characterize CTB binding to different

cell types. All of the cells were then acquired using a flow cytometer (Fortessa 20X, BD), and the data was analyzed and visualized using FlowJo 10 (Tree Star).

**Ligated Loops.** WT mice were anesthetized using isoflurane, and a midline incision was made to expose the intestine. Loops of about 3–5 cm of proximal and mid/distal small intestine were tied and injected with 10  $\mu\text{g}/\text{mL}$  CT (with or without polymer) in 100  $\mu\text{L}$  PBS + 3%  $\text{NaHCO}_3$  or just PBS + 3%  $\text{NaHCO}_3$ . The loops were reinserted into the abdomen, and the wound was closed to prevent fluid loss. After 4 h under anesthesia, the mice were sacrificed and the weight to length ratio was calculated for the loops to determine the fluid accumulation.

**Human Tissue.** Human jejunum tissue was donated after informed consent by patients undergoing gastric bypass surgery. The specimens were obtained without any information about the patients and experiments on these tissues carried according to approval from the Ethical Review Board, Gothenburg, Sweden (ethics no. 583-17). The resected tissue was immediately put in ice-cold Krebs–Ringer solution. The mucosa was dissected from the muscle and connective tissue, chopped into small pieces, and incubated 1  $\times$  25 min at 37  $^\circ\text{C}$  in HBSS (without  $\text{Ca}^{2+}$  and  $\text{Mg}^{2+}$ , Gibco, Thermo Scientific) with 5 mM EDTA, 2% FBS (Gibco, Thermo Scientific), and 15 mM HEPES (Fisher BioReagents). The tissue was then washed with HBSS without EDTA for 10 min at 37  $^\circ\text{C}$  followed by enzymatic degradation in R10 medium with Liberase (Liberase TM, Roche) and DNase I (Roche, Sigma-Aldrich) together with 5 mM  $\text{CaCl}_2$  for 45 min at 37  $^\circ\text{C}$ . The resulting fluid was filtered, washed, and stained with mAbs against EpCAM-FITC, CD45-APC-H7, and Le<sup>x</sup>-BV786 (BD Biosciences) and with CTB/LTB/OVA-biotin (conjugated with kit from Expedeon), followed by streptavidin-BV421 and live/dead marker Zombie Red (Biolegend). The blocking of CTB binding was done as above. The cells were then analyzed using flow cytometry.

**Enteroid Isolation.** Fresh tissue from human jejunum was stripped of muscle and connective tissue using scissors to isolate the mucosa. Small biopsies were then taken and treated with PBS + antibiotic-antimycotic (1:100) (Thermo Scientific) for 4  $\times$  2 min and then PBS + DTT (10 mM) for 3  $\times$  2 min. The tissue was then incubated in PBS + EDTA (2 mM), 4  $^\circ\text{C}$ , on rotation for 1 h and then violently shaken to isolate the crypts. The crypts were then seeded into matrigel (hESC-Qualified Matrix, Corning) and cultured in Intesticult (Stem Cell) to keep the cells in a stem cell state. If growing well and forming spheres after three passages, the cultures were considered to be stable enteroid lines and were used for further expansion and experiments.

**CT Challenge of Monolayers.** Stable enteroid lines were grown in matrigel for 5–7 days before breaking the spheres using a G27 needle and a syringe. The single cell suspension was then seeded onto well inserts (Corning Transwell clear polyester membrane 0.4  $\mu\text{m}$ , 0.33  $\text{cm}^2$ , Sigma-Aldrich) coated with collagen from human placenta (Sigma-Aldrich) and cultured in Intesticult (components A and B, Stem Cell) for 5–10 days to form confluent monolayers. The confluency was assessed using a microscope and measuring trans epithelial resistance (TER) with a Millicell ERS-2 V/ohm meter (Millipore). When TER reached above 600  $\Omega/\text{cm}^2$  (minus the well background resistance), the cells were grown in equal parts Intesticult component A + DMEM for 5 days to induce the differentiation of the cells into a more mature state as

previously described.<sup>42</sup> The differentiated monolayer cultures were then subjected to an apical CT challenge (0.1  $\mu\text{g}/\text{mL}$ ) where CT had been pretreated with polymers or oligosaccharides. To monitor the CT-induced ion efflux from the TER cells, the trans epithelial resistance and voltage were monitored, where the short circuit current ( $I_{\text{sc}}$ ) per  $\text{cm}^2$  was calculated. The results were then normalized to the measurements on PBS-treated cells.

## ■ ASSOCIATED CONTENT

### Supporting Information

The Supporting Information is available free of charge at <https://pubs.acs.org/doi/10.1021/acsinfecdis.0c00009>.

Monomer preparation and polymer characterization as well as flow cytometry gating strategies (PDF)

## ■ AUTHOR INFORMATION

### Corresponding Author

Ulf Yrlid – Department of Microbiology and Immunology, Institute of Biomedicine, University of Gothenburg, 405 30 Gothenburg, Sweden; Email: [ulfyrlid@gu.se](mailto:ulfyrlid@gu.se)

### Authors

Jakob Cervin – Department of Microbiology and Immunology, Institute of Biomedicine, University of Gothenburg, 405 30 Gothenburg, Sweden

Andrew Boucher – Department of Microbiology and Immunology, Institute of Biomedicine, University of Gothenburg, 405 30 Gothenburg, Sweden; [orcid.org/0000-0002-4237-4612](https://orcid.org/0000-0002-4237-4612)

Gyusaang Youn – Department of Chemistry, Stony Brook University, Stony Brook, New York 11794-3400, United States; [orcid.org/0000-0002-9152-1367](https://orcid.org/0000-0002-9152-1367)

Per Björklund – Department of Surgery, Institute of Clinical Sciences, Sahlgrenska Academy, University of Gothenburg, Sahlgrenska University Hospital/Östra, 416 85 Gothenburg, Sweden

Ville Wallenius – Department of Surgery, Institute of Clinical Sciences, Sahlgrenska Academy, University of Gothenburg, Sahlgrenska University Hospital/Östra, 416 85 Gothenburg, Sweden

Lynda Mottram – Department of Microbiology and Immunology, Institute of Biomedicine, University of Gothenburg, 405 30 Gothenburg, Sweden

Nicole S. Sampson – Department of Chemistry, Stony Brook University, Stony Brook, New York 11794-3400, United States; [orcid.org/0000-0002-2835-7760](https://orcid.org/0000-0002-2835-7760)

Complete contact information is available at: <https://pubs.acs.org/doi/10.1021/acsinfecdis.0c00009>

### Notes

The authors declare no competing financial interest.

## ■ ACKNOWLEDGMENTS

The authors thank Prof Susann Teneberg (University of Gothenburg) and Dr. Jennifer J. Kohler (University of Texas Southwestern) for invaluable help with technical questions and suggestions on writing. CTB and LTB were kindly provided by Michael Lebens and Ann-Mari Svennerholm (University of Gothenburg). We acknowledge the Centre for Cellular Imaging at the Sahlgrenska Academy, University of Gothenburg, Sweden, for the use of their imaging equipment and for

the support of their staff. This research was funded by a grant from the Swedish Research Council (2017-02646) to U.Y. and an NIH grant (R01GM097971) to N.S.S.

## REFERENCES

- (1) Ali, M., Nelson, A. R., Lopez, A. L., and Sack, D. A. (2015) Updated global burden of cholera in endemic countries. *PLoS Neglected Trop. Dis.* 9 (6), e0003832.
- (2) Clemens, J. D., Nair, G. B., Ahmed, T., Qadri, F., and Holmgren, J. (2017) Cholera. *Lancet* 390 (10101), 1539–1549.
- (3) Reboulet, S., Moore, S., Rossignol, E., Bogreau, H., Gaudart, J., Normand, A.-C., Laraque, M.-J., Adrien, P., Boncy, J., and Piarroux, R. (2019) Epidemiological and molecular forensics of cholera recurrence in Haiti. *Sci. Rep.* 9 (1), 1164.
- (4) Kennedy, J., Harmer, A., and McCoy, D. (2017) The political determinants of the cholera outbreak in Yemen. *Lancet Glob Health* 5 (10), e970–e971.
- (5) Sarkar, K. (2003) Role of oral rehydration therapy in controlling epidemic of cholera and watery diarrhoea. *J. Indian Med. Assoc.* 101 (6), 379–386.
- (6) Ray, A., Sarkar, K., Haldar, P., and Ghosh, R. (2020) Oral cholera vaccine delivery strategy in India: Routine or campaign?—A scoping review. *Vaccine* 38, A184.
- (7) Islam, M. T., Chowdhury, F., Qadri, F., Sur, D., and Ganguly, N. K. (2020) Trials of the killed oral cholera vaccine (Shanchol) in India and Bangladesh: Lessons learned and way forward. *Vaccine* 38, A127.
- (8) Merritt, E. A., and Hol, W. G. (1995) AB5 toxins. *Curr. Opin. Struct. Biol.* 5 (2), 165–171.
- (9) Holmgren, J., Lönnroth, I., and Svennerholm, L. (1973) Fixation and inactivation of cholera toxin by GM1 ganglioside. *Scand. J. Infect. Dis.* 5 (1), 77–78.
- (10) Holmgren, J., Lönnroth, I., and Svennerholm, L. (1973) Tissue receptor for cholera exotoxin: postulated structure from studies with GM1 ganglioside and related glycolipids. *Infect. Immun.* 8 (2), 208–214.
- (11) Merritt, E. A., Sarfaty, S., van den Akker, F., L'Hoir, C., Martial, J. A., and Hol, W. G. (1994) Crystal structure of cholera toxin B-pentamer bound to receptor GM1 pentasaccharide. *Protein Sci.* 3 (2), 166–175.
- (12) Holmgren, J., Lönnroth, I., Månsson, J., and Svennerholm, L. (1975) Interaction of cholera toxin and membrane GM1 ganglioside of small intestine. *Proc. Natl. Acad. Sci. U. S. A.* 72 (7), 2520–2524.
- (13) Kumar, V., and Turnbull, W. B. (2018) Carbohydrate inhibitors of cholera toxin. *Beilstein J. Org. Chem.* 14 (1), 484–498.
- (14) Bernardi, A., Carrettoni, L., Ciponte, A. G., Monti, D., and Sonnino, S. (2000) Second generation mimics of ganglioside GM1 as artificial receptors for cholera toxin: replacement of the sialic acid moiety. *Bioorg. Med. Chem. Lett.* 10 (19), 2197–2200.
- (15) Bernardi, A., Checchia, A., Brocca, P., Sonnino, S., and Zuccotto, F. (1999) Sugar Mimics: An Artificial Receptor for Cholera Toxin. *J. Am. Chem. Soc.* 121 (10), 2032–2036.
- (16) Arosio, D., Vrasidas, I., Valentini, P., Liskamp, R. M. J., Pieters, R. J., and Bernardi, A. (2004) Synthesis and cholera toxin binding properties of multivalent GM1 mimics. *Org. Biomol. Chem.* 2 (14), 2113–12.
- (17) Pukin, A. V., Branderhorst, H. M., Sisu, C., Weijers, C. A. G. M., Gilbert, M., Liskamp, R. M. J., Visser, G. M., Zuilhof, H., and Pieters, R. J. (2007) Strong Inhibition of Cholera Toxin by Multivalent GM1 Derivatives. *ChemBioChem* 8 (13), 1500–1503.
- (18) Branderhorst, H. M., Liskamp, R. M. J., Visser, G. M., and Pieters, R. J. (2007) Strong inhibition of cholera toxin binding by galactose dendrimers. *Chem. Commun. (Cambridge, U. K.)* 81 (47), 5043–5045.
- (19) Das, S., Angsantikul, P., Le, C., Bao, D., Miyamoto, Y., Gao, W., Zhang, L., and Eckmann, L. (2018) Neutralization of cholera toxin with nanoparticle decoys for treatment of cholera. *PLoS Neglected Trop. Dis.* 12 (2), e0006266.
- (20) Haksar, D., de Poel, E., van Ufford, L. Q., Bhatia, S., Haag, R., Beekman, J., and Pieters, R. J. (2019) Strong Inhibition of Cholera Toxin B Subunit by Affordable, Polymer-Based Multivalent Inhibitors. *Bioconjugate Chem.* 30, 785.
- (21) Zomer-van Ommen, D. D., Pukin, A. V., Fu, O., Quarles van Ufford, L. H. C., Janssens, H. M., Beekman, J. M., and Pieters, R. J. (2016) Functional Characterization of Cholera Toxin Inhibitors Using Human Intestinal Organoids. *J. Med. Chem.* 59 (14), 6968–6972.
- (22) Breimer, M. E., Hansson, G. C., Karlsson, K. A., Larson, G., and Leffler, H. (2012) Glycosphingolipid composition of epithelial cells isolated along the villus axis of small intestine of a single human individual. *Glycobiology* 22 (12), 1721–1730.
- (23) Pongkorpsakol, P., Pathomthongtawecheai, N., Srimanote, P., Soodvilai, S., Chatsudthipong, V., and Muanprasat, C. (2014) Inhibition of cAMP-activated intestinal chloride secretion by diclofenac: cellular mechanism and potential application in cholera. *PLoS Neglected Trop. Dis.* 8 (9), e3119.
- (24) Pongkorpsakol, P., Wongkrasant, P., Kumpun, S., Chatsudthipong, V., and Muanprasat, C. (2015) Inhibition of intestinal chloride secretion by piperine as a cellular basis for the anti-secretory effect of black peppers. *Pharmacol. Res.* 100, 271–280.
- (25) Wolf, A. A., Fujinaga, Y., and Lencer, W. I. (2002) Uncoupling of the cholera toxin-G(M1) ganglioside receptor complex from endocytosis, retrograde Golgi trafficking, and downstream signal transduction by depletion of membrane cholesterol. *J. Biol. Chem.* 277 (18), 16249–16256.
- (26) Fullner, K. J., Lencer, W. I., and Mekalanos, J. J. (2001) Vibrio cholerae-Induced Cellular Responses of Polarized T84 Intestinal Epithelial Cells Are Dependent on Production of Cholera Toxin and the RTX Toxin. *Infect. Immun.* 69 (10), 6310–6317.
- (27) Heggelund, J. E., Burschowsky, D., Bjørnstad, V. A., Hodnik, V., Anderluh, G., and Kregel, U. (2016) High-Resolution Crystal Structures Elucidate the Molecular Basis of Cholera Blood Group Dependence. *PLoS Pathog.* 12 (4), e1005567–19.
- (28) Vasile, F., Reina, J. J., Potenza, D., Heggelund, J. E., Mackenzie, A., Kregel, U., and Bernardi, A. (2014) Comprehensive analysis of blood group antigen binding to classical and El Tor cholera toxin B-pentamers by NMR. *Glycobiology* 24 (8), 766–778.
- (29) Cervin, J., Wands, A. M., Casselbrant, A., Wu, H., Krishnamurthy, S., Cvjetkovic, A., Estelius, J., Dedic, B., Sethi, A., Wallom, K.-L., et al. (2018) GM1 ganglioside-independent intoxication by Cholera toxin. *PLoS Pathog.* 14 (2), e1006862.
- (30) Wang, H., Ng, T. B., Ooi, V. E., and Liu, W. K. (2000) Effects of lectins with different carbohydrate-binding specificities on hepatoma, choriocarcinoma, melanoma and osteosarcoma cell lines. *Int. J. Biochem. Cell Biol.* 32 (3), 365–372.
- (31) Haksar, D., Quarles van Ufford, L., and Pieters, R. J. (2020) A hybrid polymer to target blood group dependence of cholera toxin. *Org. Biomol. Chem.* 18 (1), 52–55.
- (32) Stowell, S. R., Ju, T., and Cummings, R. D. (2015) Protein glycosylation in cancer. *Annu. Rev. Pathol.: Mech. Dis.* 10 (1), 473–510.
- (33) Very, N., Lefebvre, T., and El Yazidi-Belkoura, I. (2018) Drug resistance related to aberrant glycosylation in colorectal cancer. *Oncotarget* 9 (1), 1380–1402.
- (34) Wu, L., and Sampson, N. S. (2014) Fucose, mannose, and  $\beta$ -N-acetylglucosamine glycopolymers initiate the mouse sperm acrosome reaction through convergent signaling pathways. *ACS Chem. Biol.* 9 (2), 468–475.
- (35) Heggelund, J. E., Haugen, E., Lygren, B., Mackenzie, A., Holmner, Å., Vasile, F., Reina, J. J., Bernardi, A., and Kregel, U. (2012) Both El Tor and classical cholera toxin bind blood group determinants. *Biochem. Biophys. Res. Commun.* 418 (4), 731–735.
- (36) Carpenter, C. C., Sack, R. B., Feeley, J. C., and Steenberg, R. W. (1968) Site and characteristics of electrolyte loss and effect of intraluminal glucose in experimental canine cholera. *J. Clin. Invest.* 47 (5), 1210–1220.



- (37) Carpenter, C. C., and Greenough, W. B. (1968) Response of the canine duodenum to intraluminal challenge with cholera exotoxin. *J. Clin. Invest.* 47 (12), 2600–2607.
- (38) Banwell, J. G., Pierce, N. F., Mitra, R. C., Brigham, K. L., Caranasos, G. J., Keimowitz, R. I., Fedson, D. S., Thomas, J., Gorbach, S. L., Sack, R. B., et al. (1970) Intestinal fluid and electrolyte transport in human cholera. *J. Clin. Invest.* 49 (1), 183–195.
- (39) Holmgren, J., Lindblad, M., Fredman, P., Svennerholm, L., and Myrvold, H. (1985) Comparison of receptors for cholera and Escherichia coli enterotoxins in human intestine. *Gastroenterology* 89 (1), 27–35.
- (40) Fukuta, S., Magnani, J. L., Twiddy, E. M., Holmes, R. K., and Ginsburg, V. (1988) Comparison of the carbohydrate-binding specificities of cholera toxin and Escherichia coli heat-labile enterotoxins LT-I, LT-IIa, and LT-IIb. *Infect. Immun.* 56 (7), 1748–1753.
- (41) Teneberg, S., Hirst, T. R., Ångström, J., and Karlsson, K.-A. (1994) Comparison of the glycolipid-binding specificities of cholera toxin and porcine Escherichia coli heat-labile enterotoxin: identification of a receptor-active non-ganglioside glycolipid for the heat-labile toxin in infant rabbit small intestine. *Glycoconjugate J.* 11 (6), 533–540.
- (42) Noel, G., Baetz, N. W., Staab, J. F., Donowitz, M., Kovbasnjuk, O., Pasetti, M. F., and Zachos, N. C. (2017) A primary human macrophage-enteroid co-culture model to investigate mucosal gut physiology and host-pathogen interactions. *Sci. Rep.* 7, 45270.
- (43) Sethi, A., Wands, A. M., Mettlen, M., Krishnamurthy, S., Wu, H., and Kohler, J. J. (2019) Cell type and receptor identity regulate cholera toxin subunit B (CTB) internalization. *Interface Focus* 9 (2), 20180076.
- (44) Wands, A. M., Fujita, A., McCombs, J. E., Cervin, J., Dedic, B., Rodriguez, A. C., Nischan, N., Bond, M. R., Mettlen, M., Trudgian, D. C., et al. (2015) Fucosylation and protein glycosylation create functional receptors for cholera toxin. *eLife* 4, e09545.
- (45) Matsumura, K., Higashida, K., Ishida, H., Hata, Y., Yamamoto, K., Shigeta, M., Mizuno-Horikawa, Y., Wang, X., Miyoshi, E., Gu, J., et al. (2007) Carbohydrate binding specificity of a fucose-specific lectin from *Aspergillus oryzae*: a novel probe for core fucose. *J. Biol. Chem.* 282 (21), 15700–15708.
- (46) Choi, H.-K., Lee, D., Singla, A., Kwon, J. S.-I., and Wu, H.-J. (2019) The influence of heteromultivalency on lectin-glycan binding behavior. *Glycobiology* 29 (5), 397–408.
- (47) Kuhlmann, F. M., Santhanam, S., Kumar, P., Luo, Q., Ciorba, M. A., and Fleckenstein, J. M. (2016) Blood Group O-Dependent Cellular Responses to Cholera Toxin: Parallel Clinical and Epidemiological Links to Severe Cholera. *Am. J. Trop. Med. Hyg.* 95 (2), 440–443.
- (48) Cohen, M. B., Giannella, R. A., Losonsky, G. A., Lang, D. R., Parker, S., Hawkins, J. A., Gunther, C., and Schiff, G. A. (1999) Validation and characterization of a human volunteer challenge model for cholera by using frozen bacteria of the new *Vibrio cholerae* epidemic serotype, O139. *Infect. Immun.* 67 (12), 6346–6349.
- (49) Glass, R. I., Holmgren, J., Haley, C. E., Khan, M. R., Svennerholm, A. M., Stoll, B. J., Belayet Hossain, K. M., Black, R. E., Yunus, M., and Barua, D. (1985) Predisposition for cholera of individuals with O blood group. Possible evolutionary significance. *Am. J. Epidemiol.* 121 (6), 791–796.
- (50) Hornick, R. B., Music, S. I., Wenzel, R., Cash, R., Libonati, J. P., Snyder, M. J., and Woodward, T. E. (1971) The Broad Street pump revisited: response of volunteers to ingested cholera vibrios. *Bull. N Y Acad. Med.* 47 (10), 1181–1191.
- (51) Love, J. A., Morgan, J. P., Trnka, T. M., and Grubbs, R. H. (2002) A practical and highly active ruthenium-based catalyst that effects the cross metathesis of acrylonitrile. *Angew. Chem., Int. Ed.* 41 (21), 4035–4037.
- (52) Lebens, M., Johansson, S., Osek, J., Lindblad, M., and Holmgren, J. (1993) Large-scale production of *Vibrio cholerae* toxin B subunit for use in oral vaccines. *Nat. Biotechnol.* 11 (13), 1574–1578.
- (53) Sheikh, K. A., Sun, J., Liu, Y., Kawai, H., Crawford, T. O., Proia, R. L., Griffin, J. W., and Schnaar, R. L. (1999) Mice lacking complex gangliosides develop Wallerian degeneration and myelination defects. *Proc. Natl. Acad. Sci. U. S. A.* 96 (13), 7532–7537.
- (54) Takamiya, K., Yamamoto, A., Yamashiro, S., Shin, M., Okada, M., Fukumoto, S., Haraguchi, M., Takeda, N., Fujimura, K., Sakae, M., et al. (1996) Mice with disrupted GM2/GD2 synthase gene lack complex gangliosides but exhibit only subtle defects in their nervous system. *Proc. Natl. Acad. Sci. U. S. A.* 93 (20), 10662–10667.
- (55) Sun, J., Shaper, N. L., Itonori, S., Heffer-Lauc, M., Sheikh, K. A., and Schnaar, R. L. (2004) Myelin-associated glycoprotein (Siglec-4) expression is progressively and selectively decreased in the brains of mice lacking complex gangliosides. *Glycobiology* 14 (9), 851–857.